1997

VLBI Observations of the Gamma-Ray Blazar 1611+343

B. Glenn Piner
Whittier College, gpiner@whittier.edu

Kerry A. Kingham

THE ASTROPHYSICAL JOURNAL, 479:684–693, 1997 April 20

VLBI OBSERVATIONS OF THE GAMMA-RAY BLAZAR 1611+343

B. GLENN PINER[1,2] AND KERRY A. KINGHAM
US Naval Observatory, Earth Orientation Department, 3450 Massachussets Avenue, Washington, DC 20392
Received 1996 August 14; accepted 1996 November 13

ABSTRACT

As part of an effort to observe high-energy γ-ray blazars with VLBI, we have produced 8 and 2 GHz VLBI images, at eight epochs, of the quasar 1611+343, which has been detected by the EGRET telescope on board the *Compton Gamma Ray Observatory*. The VLBI data have been taken from the geodetic database of the Washington VLBI correlator. As is expected for a γ-ray quasar, we find that 1611+343 possesses a jet with several compact components moving at apparent superluminal speeds. We have detected five components and have measured speeds for the outer four of 6.7 ± 1.6, 3.8 ± 1.4, 7.6 ± 1.3, and 11.5 ± 2.3 $h^{-1}c$ from the outermost component inward. ($H_0 = 100$ h km s^{-1} Mpc^{-1}, $q_0 = 0.5$.) By comparing the apparent superluminal expansion speeds with a lower limit to the Doppler beaming factor derived from X-ray observations, we have calculated an upper limit on the angle of the jet to the line of sight of $\theta \leq 6.^{\circ}8$ and a lower limit to the Lorentz factor of the components of $\Gamma \geq 7.1$. We have mapped the two-dimensional projected structure of the VLBI jet and clearly see different trajectories for different components at the same distance from the core, which rules out a continuous jet model for this source. A possible connection is found between enhanced levels of γ-ray activity and the ejection of new VLBI components from the core.

Subject headings: galaxies: jets — galaxies: kinematics and dynamics — galaxies: structure — gamma rays: theory — quasars: individual (1611+343) — radio continuum: galaxies

1. INTRODUCTION

Since its launch in 1991, the EGRET instrument on board the *Compton Gamma Ray Observatory* (*CGRO*) has detected with high significance 40 blazars as emitters of high-energy γ-rays (Thompson et al. 1995; von Montigny et al. 1995). If the γ-rays are produced in a beamed relativistic jet, these sources should show distinct properties such as apparent superluminal motion and, indeed, several do. Some of these blazars were known superluminals before their detection by EGRET, and superluminal motion has been confirmed in others since their EGRET detection (see § 5.4). Quasar 1611+343 is the fifteenth EGRET source to display apparent superluminal motion, and it is expected that all EGRET blazars will show this property if examined sufficiently closely. This paper represents the first step in a project to study as many EGRET sources as possible which have not been previously well observed with VLBI, using the geodetic VLBI database of the Washington VLBI correlator.

This paper also demonstrates the utility of using archived geodetic VLBI observations to obtain results of astrophysical importance. Geodetic VLBI observations have been used for astronomical projects several times (e.g., Charlot 1990; Britzen et al. 1994), although these projects have tended to concentrate on analyzing a single experiment or following a single source over time. The project of which this paper is a part will attempt to study about a dozen sources through many archived experiments. An advantage of using archived geodetic observations is that for the few very well observed sources an almost arbitrarily fine time sampling can be obtained, although images may not be of high quality. This is of particular value for such applications as mapping out the geometry of the jet, which is done for 1611+343 in § 5.3. We discuss previous observations of 1611+343 in § 2, the archived geodetic VLBI observations in § 3, the component motions in § 4, and other astrophysical results in § 5.

2. PREVIOUS OBSERVATIONS OF 1611+343

The source 1611+343 is an optically violent variable (OVV) quasar with a redshift of $z = 1.4$ (Hewitt & Burbidge 1989). It is a flat spectrum radio source with an average spectral index measured with the Green Bank interferometer of $\alpha = -0.04$ between 2.7 and 8.1 GHz during the time period 1990 to 1995 (Waltman 1996, private communication) , where α is defined by $S \propto \nu^{\alpha}$. The radio variability of this quasar has been monitored with the Green Bank interferometer at 8.1 and 2.7 GHz since 1983 (Waltman et al. 1991), by the Michigan group at 4.8, 8.0, and 14.5 GHz since 1980 (Aller et al. 1985), and by the Metsähovi group at 22 and 37 GHz since 1990 (Valtaoja 1996, private communication). The only prominent radio outburst seen in this data starts around 1993 and peaks around 1995 January. Optical monitoring of this quasar from 1983 to 1988, which shows an outburst occuring between 1986 October and 1987 March, is reported in Tornikoski et al. (1994). The optical polarization has been reported by Rusk & Seaquist (1985) as $1.68 \pm 0.27\%$ along a position angle of $134^{\circ} \pm 11^{\circ}$ making 1611+343 a low-polarization quasar (LPQ). Rusk (1988) presents a VLA image at 1.375 GHz which shows 1611+343 to have a southern extension along a position angle of 197°. A high dynamic range VLA image at 1.64 GHz, presented by Murphy, Browne, & Perley (1993), shows that 1611+343 exhibits a triple morphology where the position angle of the brighter southern component is consistent with the southern extension discussed by Rusk. The source is core dominated with a core fraction of greater than 99% at 1.64 GHz. Evidence for a compact core also comes from the fact that 1611+343 is an extreme scattering event source as reported by Fiedler et al. (1994).

[1] Department of Astronomy, University of Maryland, College Park, MD 20742.
[2] NASA/Goddard Space Flight Center, Code 661, Greenbelt, MD 20771.

1611+343 was observed with VLBI at 5 GHz in a three-antenna experiment by Zensus, Porcas, & Pauliny-Toth (1984). It was well fitted by a circular Gaussian of width 0.6 mas. This quasar has also been imaged with lower frequency VLBI at several epochs as part of a campaign to study the milliarcsecond-scale structure of low-frequency variable sources (Romney et al. 1984; Padrielli et al. 1986, 1991; Bondi et al. 1996). These observations all showed 1611+343 to be compact and well modeled by a single component. Other VLBI observations are given by Bååth (1987) at 932 MHz and by Waak et al. (1988) at 1.66 GHz with resolutions of about 5 and 10 mas, respectively. The source structure is unresolved in both cases. None of these previous VLBI observations has had the resolution needed to resolve the core-jet structure of this source.

The high-energy γ-ray telescope EGRET has observed 1611+343 on five separate occasions and found that like other γ-ray blazars, it is highly variable. It was in a quiescent state prior to 1992 and yielded only upper limits when observed by EGRET in 1991 September and 1992 April. It was found to be in an enhanced state of activity when observed in 1992 November and has continued to show higher levels of γ-ray activity in subsequent observations, with fluxes of 44 ± 8, 47 ± 26, and $69 \pm 15 \times 10^{-8}$ photons cm^{-2} s^{-1} (greater than 100 MeV) being recorded in 1992 November, 1993 October, and 1994 November, respectively (Thompson et al. 1995; EGRET team 1996, private communication). A χ^2 test shows that the probability that the flux was constant during all of these observations is only 8.9×10^{-7}. The level of γ-ray activity definitely increased sometime between 1992 April and 1992 November, whether the subsequent high levels of activity represent individual flares or a constant higher level of activity cannot be determined because of the poor time sampling of the EGRET light curve.

3. VLBI OBSERVATIONS

The VLBI observations used in this paper are from archived geodetic Mark III VLBI observations (Rogers et al. 1983; Clark et al. 1985; Rogers et al. 1993), processed at the Washington VLBI Correlator Facility located at the Naval Observatory (USNO); and obtained by the Naval Observatory (Eubanks et al. 1991), National Oceanographic and Atmospheric Administration (Carter, Robertson, & MacKay 1985), and by NASA's Crustal Dynamics Project (Coates et al. 1985; Smith & Turcotte 1993) and its successor, the Space Geodesy Project. Observations are done at eight separate intermediate frequencies between 8 and 9 GHz, and six separate intermediate frequencies between 2 and 3 GHz, and these intermediate frequencies are retained as separate (u, v) plane points. An integration time of 4 s is used for each (u, v) plane point. The strength of this database is the large number of observations; the observations started in 1986 and several sources have over 1000 observations up to the present. A drawback is that since the observations were not designed for imaging, many of them have poor (u, v) plane coverage. This can be compensated for by adding together observations which were close together in time; this can be done as long as there is enough data per observation to perform self-calibration separately on each observation, and as long as separate flux density data show that the source was approximately constant over the time span of the summed observations. For this paper we have summed observations with time differences of no more than 42 days; we have verified that the radio flux density of 1611+343 was constant over these times (Waltman 1996, private communication), and we have performed self-calibration separately on each observation to be summed. The data were calibrated and fringed using standard routines from the AIPS software package, and images were produced using standard self-calibration procedures (e.g., Pearson & Readhead 1984) from the Caltech Difmap software package.

We have imaged 1611+343 at eight different epochs; 1990 July 23, 1992 July 19, 1993 July 8, 1994 January 18, 1994 December 13, 1995 January 24, 1995 October 17, and 1996 March 26. Images for the first three epochs were produced by summing separate observations, with four, five, and four separate observations being summed for these first three epochs, respectively. The times of the individual observations which were summed to produce images for the first three epochs were 1990 July 11, 1990 July 20, 1990 July 26, and 1990 August 20 for the first epoch; 1992 June 29, 1992 July 13, 1992 July 21, 1992 August 3, and 1992 August 10 for the second epoch; and 1993 June 24, 1993 June 25, 1993 July 16, and 1993 July 21 for the third epoch. The time coordinates used for the first three epochs are the averages of the times of the individual observations, weighted by the number of measured visibilities per observation. The antennas used in all observations are listed in Table 1.

The 8 GHz radio images are presented in Figures 1*a*–1*h*, and a typical 2 GHz image from epoch 1994 January 18 is

TABLE 1

ANTENNAS USED IN THE OBSERVATIONS

Antenna Location	Size (m)	Epochs[a]
Algonquin, ON, Canada	46	1c, 2de, 3a, 7
Brewster, WA	25	4
Fairbanks, AK	26	1bd, 2abc, 3ad, 4, 5, 6, 7, 8
Fortaleza, Brazil	14	4, 5, 6, 7, 8
Goldstone, CA	34	2a
Goldstone, CA	26	1d
Goldstone, CA	12	1abc, 2bde
Greenbank, WV	26	3a, 4, 5, 6
Greenbank, WV	20	7, 8
Hancock, NH	25	3b
Hartebeesthoek, South Africa	26	2c, 3bcd
Hobart, Tasmania	26	1b, 2c, 3c
Kashima, Japan	34	1bd
Kashima, Japan	26	2ac, 3cd
Kauai, HI	9	2c
Kauai, HI	20	3d, 4, 5, 6, 7, 8
Madrid, Spain	34	3b
Matera, Italy	20	3a
Mauna Kea, HI	25	4, 7
Medicina, Italy	32	1d, 2a
Nobeyama, Japan	6	1b
North Liberty, IA	25	7
Ny Alesund, Norway	20	5, 8
Onsala, Sweden	20	1ad, 2a, 3a
Perrine, FL	18	1ac, 2bde
St. Croix, USVI	25	3b, 4
Santiago, Chile	12	2c, 3bd
Shanghai, China	25	2c, 3c
Tidbinbilla, Australia	34	3c
Westford, MA	37	1d, 2a
Westford, MA	18	1ac, 2bcde, 3d
Wettzell, Germany	20	1ac, 2bcde, 3acd, 4, 5, 6, 7, 8

[a] Epochs 1–8 refer to times 1990 July 23, 1992 July 19, 1993 July 8, 1994 January 18, 1994 December 13, 1995 January 24, 1995 October 17, and 1996 March 26, respectively. The letters a, b, c, d, e after the epoch numbers refer to different observations within the overall summed observation.

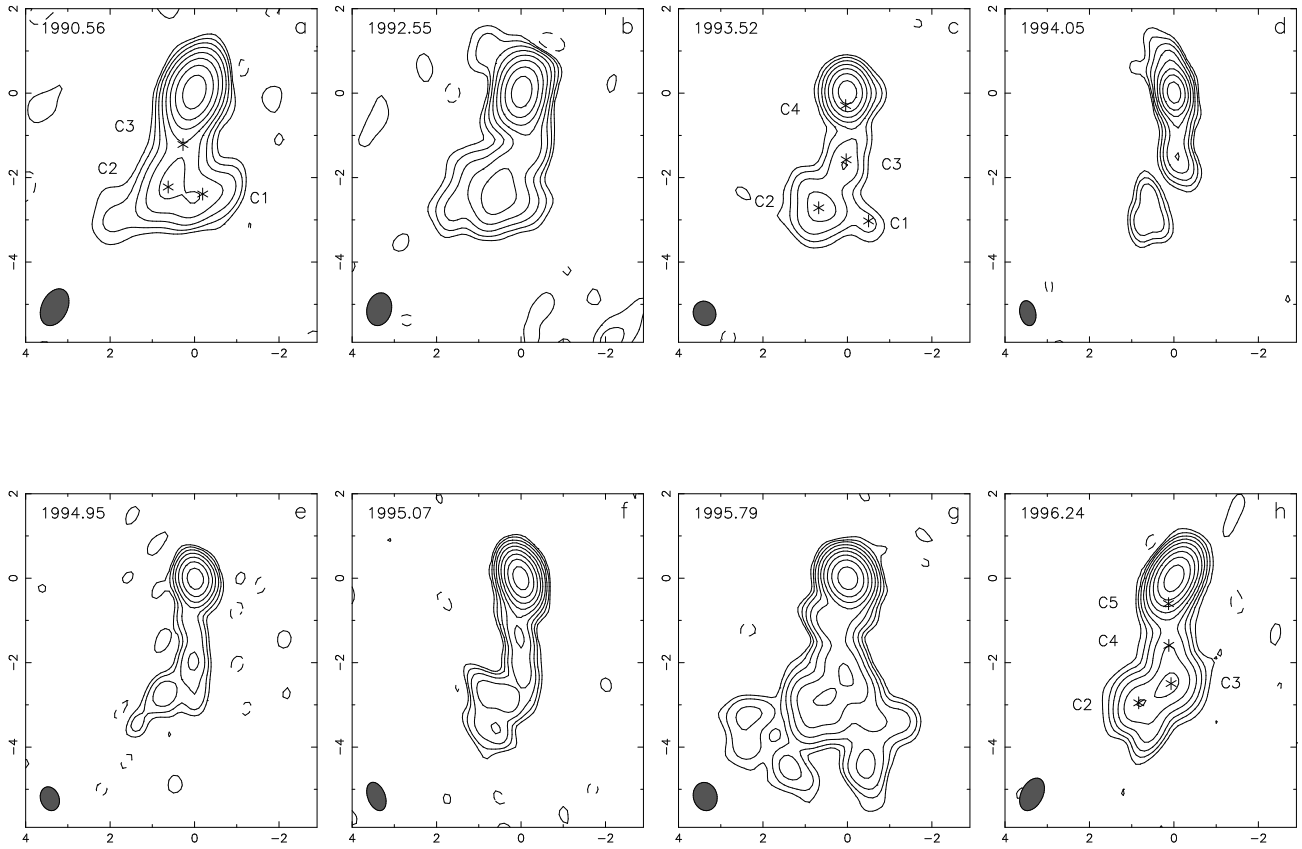

FIG. 1.—(*a*)–(*h*): 8 GHz VLBI images of 1611+343. Relative right ascension and declination are plotted with tickmark spacings of 1 mas. Contour levels are −1%, 1%, 2%, 4%, 8%, 16%, 32%, and 64% of the peak brightness. (*a*), (*b*), and (*d*) have extra contours at ±0.5%; (*f*) and (*g*) have extra contours at ±0.25% and 0.5%; and (*h*) has extra contours at ±0.2% and 0.5%. The respective FWHMs in milliarcseconds and position angles of the restoring beams are 0.93 × 0.61 at 26°, 0.79 × 0.58 at 14°, 0.59 × 0.53 at 24°, 0.60 × 0.37 at 13°, 0.58 × 0.44 at 20°, 0.70 × 0.41 at 21°, 0.68 × 0.56 at 16°, and 0.82 × 0.51 at 27°. The peak brightness levels are 1.77, 2.14, 1.61, 1.27, 1.95, 1.64, 2.01, and 1.83 Jy beam^{-1}, respectively. At least one negative contour is shown in each image. The centers of the fitted component positions are marked with asterisks in the first image, and also in the images in which C4 and C5 first appear.

presented in Figure 2. A coherent integration time of 4 s was used for each of the images except for Figure 1*g*, where the data were averaged over 16 s intervals. The dynamic range of the images ranges from 100:1 to 500:1 and the typical resolution is about 0.5 mas for the 8 GHz images. The 8 GHz images clearly show a complex jet structure extending southward from the presumed core. The inner part of this structure is misaligned by only 18° from the arcsecond-scale structure, making 1611+343 an aligned source, as is expected for a low-polarization quasar (Xu et al. 1994). The major features are present through all of the images; much of the difference in appearance from image to image is due to the differing (*u*, *v*) plane coverage of each observation. For example, Figure 1*g* brings out more of the extended low flux density emission because that observation had an unusually short baseline from Mauna Kea to Kauai. In the 2 GHz image the jet dominates the emission, while the presumed core can be seen as a northern extension. Values for the spectral indices of the presumed core and jet can be calculated by summing the fluxes for the model components which were fitted to the 8 and 2 GHz images (see § 4). We have calculated errors in the absolute flux density values of 8% for the 8 GHz images and 20% for the 2 GHz images, based on radio light curves for other sources in the experiments (Waltman 1996, private communication). The average value for the spectral index of the presumed core for these eight images is $\alpha = 0.75 \pm 0.07$, and the average value for the spectral index of the southern extension is $\alpha = -0.82 \pm 0.09$. Since it is expected that the quasar core should have a flatter spectrum (Zensus & Pearson 1988), this supports the identification of the northern component as the core. The average spectral index for the entire image is $\alpha = -0.09 \pm 0.07$, consistent with the average spectral index measured with the Green Bank interferometer of $\alpha = -0.04$.

4. MOTION IN 1611+343

In this section we investigate the motion of the components in the jet of 1611+343 relative to the core, which appears to remain stationary from data in the USNO astrometric solution (Piner & Kingham 1997). In order to quantify the positions and motions of the jet components, we fit Gaussian models to the observed visibilities for each epoch. The fitted components were either elliptical Gaussians, circular Gaussians, or point sources. Elliptical Gaussians were fitted where possible; if the axial ratio of the ellipses became less than 0.1 then circular Gaussians were used instead; if the size of the circular component became smaller than one-tenth of a beam then a point source was used. Table 2 lists the fluxes and positions of the major components of the best-fitting model for each image. In addition to the presumed core (hereafter C0), there are several jet components present in each image. The outermost component, C1, is visible only in the first three epochs

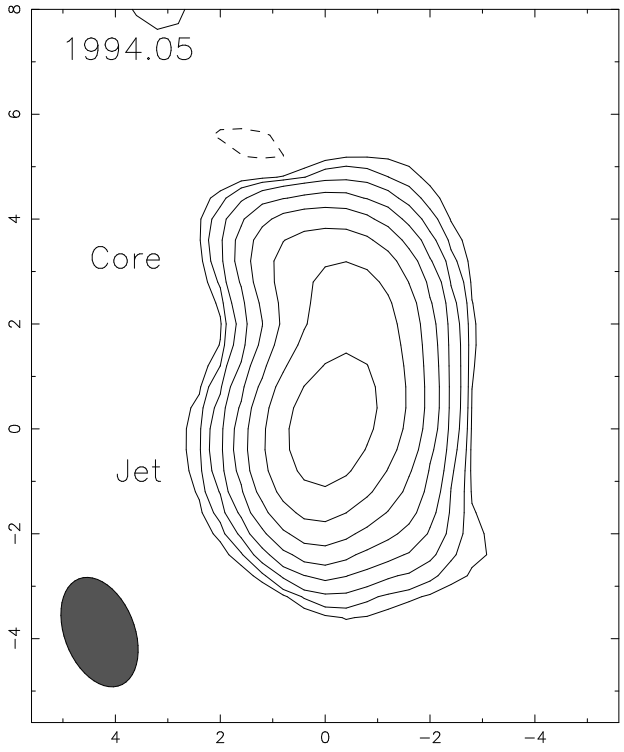

FIG. 2.—2 GHz VLBI image of 1611+343 at 1994 January 18. This image is typical of the other 2 GHz images. Note that the jet dominates the emission at this frequency and is placed at the origin. Contour levels are −0.5%, 0.5%, 1%, 2%, 4%, 8%, 16%, 32%, and 64% of the peak brightness of 1.24 Jy beam^{-1}. The FWHMs in milliarcseconds and position angle of the restoring beam are 2.18 × 1.34 at 21°.

and then again in the image from the 1995 October 17 experiment, which had increased sensitivity as well as some shorter baselines. Moving inward, there are two jet components which are present in every image; hereafter they will be referred to as C2 and C3 for the outer and inner component, respectively. At epoch 1993 July 8 a new component, C4, has appeared between C3 and the core and in the last image from 1996 March 26 a new component, C5, has appeared between C4 and the core.

Figure 3 shows the motions of the components over time. The error in the component positions is taken to be one-fourth of the beam FWHM along the direction from the core to the component's center. This assumed error is consistent with the different values obtained for component positions between the adjacent epochs 1994 December 13 and 1995 January 24. Note that although it appears from this figure that the two outermost components are initially right on top of each other, they are in fact at quite different position angles and therefore easy to distinguish. If we assume that the components move with constant velocity, then performing a least-squares fit of component positions to a straight line gives the apparent velocities of separation. The velocities obtained are 6.7 ± 1.6, 3.8 ± 1.4, 7.6 ± 1.3, and $11.5 \pm 2.3\ h^{-1}c$ for C1 to C4, respectively. ($H_0 = 100\ h$ km s^{-1} Mpc^{-1}, $q_0 = 0.5$). These speeds fall in the typical range of measured speeds for superluminal sources, although the measured speed for C4 is at the high end of this range (Vermeulen & Cohen 1994). No velocity can be measured for the innermost component since it has only been seen at one epoch. The hypothesis that all components have the same apparent speed is rejected with 97.4% con-

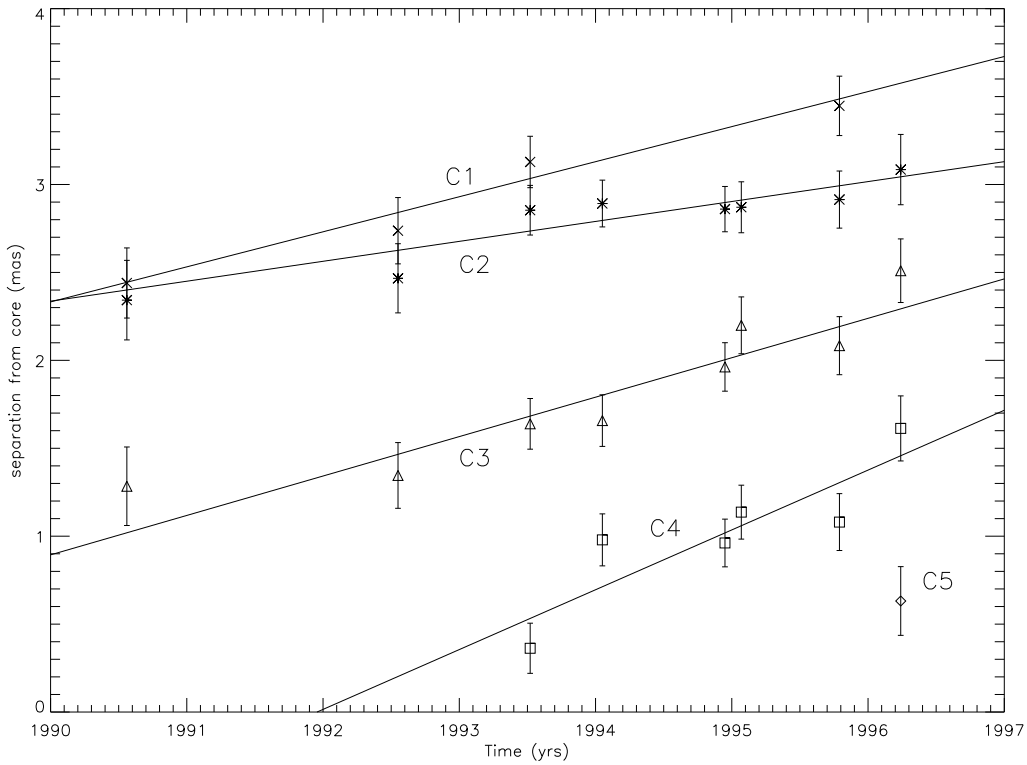

FIG. 3.—Motion of components in 1611+343. The vertical axis shows the separation in mas of the center of the component from the presumed core. The straight lines represent the best fit of the data to motion with constant velocity. The crosses represent component C1, the asterisks C2, the triangles C3, the squares C4, and the diamond C5. The error bars are one-fourth of the beam FWHM in the direction from the core to the component.

TABLE 2

GAUSSIAN MODELS

Epoch	Component	S[a] (Jy)	r[b] (mas)	θ (deg)	a[c] (mas)	b/a	Φ[d] (deg)
1990 July 23.....	C0	2.11	0.00	0.00	0.47	0.35	2.6
	C3	0.12	1.28	167.82	0.17	...	...
	C2	0.32	2.34	164.69	0.76	...	...
	C1	0.19	2.44	184.65	0.72	...	...
1992 July 19.....	C0	2.65	0.00	0.00	0.51	0.34	−3.1
	C3	0.20	1.35	186.47	0.39	...	...
	C2	0.67	2.47	166.48	0.94	0.75	−20.7
	C1	0.06	2.74	184.92	...	...	...
1993 July 8	C0	1.72	0.00	0.00	0.30	0.27	−1.0
	C4	0.26	0.36	172.82	0.25	...	...
	C3	0.30	1.64	178.87	1.01	0.40	−16.8
	C2	0.54	2.85	166.22	0.86	0.89	5.7
	C1	0.04	3.13	189.16	...	...	...
1994 January 18	C0	1.45	0.00	0.00	0.31	0.33	−7.8
	C4	0.10	0.98	185.14	...	...	...
	C3	0.11	1.66	183.27	0.23	...	...
	C2	0.18	2.89	168.28	1.12	0.37	−8.9
1994 December 13.....	C0	2.31	0.00	0.00	0.31	0.46	−12.8
	C4	0.21	0.96	174.11	0.47	...	...
	C3	0.34	1.96	178.33	0.44	...	...
	C2	0.15	2.86	164.01	0.20	...	...
1995 January 24	C0	1.81	0.00	0.00	0.23	0.46	−24.0
	C4	0.21	1.14	177.50	1.22	0.14	6.6
	C3	0.11	2.20	183.37	0.39	...	...
	C2	0.11	2.87	171.63	0.56	...	...
1995 October 17.....	C0	2.09	0.00	0.00	0.18	0.72	42.9
	C4	0.19	1.08	168.49	0.48	...	...
	C3	0.21	2.08	176.01	0.37	...	...
	C2	0.74	2.91	169.90	1.51	0.47	−72.6
	C1	0.15	3.45	192.01	0.76	...	...
1996 March 26.....	C0	1.82	0.00	0.00	0.10	0.30	−51.7
	C5	0.10	0.63	167.87	0.24	...	...
	C4	0.07	1.61	175.52	...	...	...
	C3	0.28	2.51	178.34	0.47	...	...
	C2	0.19	3.08	164.24	0.47	0.46	55.3

[a] Flux density in Janskys.

[b] r and θ are the polar coordinates of the center of the component relative to the presumed core C0. Polar angle is measured from north through east.

[c] a and b are the FWHM of the major and minor axes of the Gaussian component.

[d] Position angle of the major axis measured from north through east.

fidence. The measurements suggest that the apparent expansion speeds are greater for the inner components; this could be caused by differing bulk Lorentz factors or differing angles to the line of sight for the different components.

The component motions are easier to see when the images are presented in a mosaic plot such as Figure 4. This figure shows the component positions superimposed over a selection of five images which are spaced horizontally according

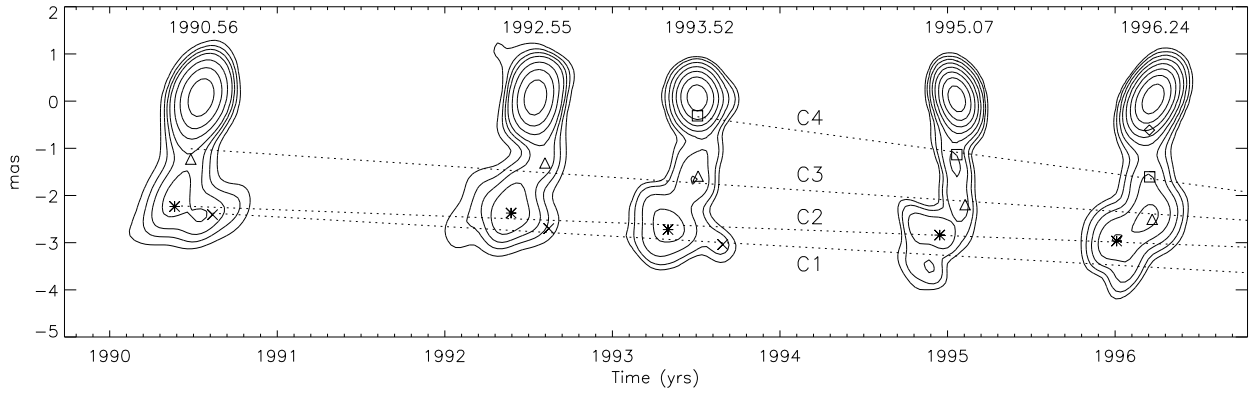

FIG. 4.—Mosaic plot of images and component motions. Time is plotted along the horizontal axis and relative declination is plotted along the vertical axis. Only five images can be shown because of size constraints. The images presented are from 1990 July 23, 1992 July 19, 1993 July 8, 1995 January 24, and 1996 March 26. Component positions are plotted on top of the images and the dotted lines show the best fit to the component motions. The crosses represent component C1, the asterisks C2, the triangles C3, the squares C4, and the diamond C5.

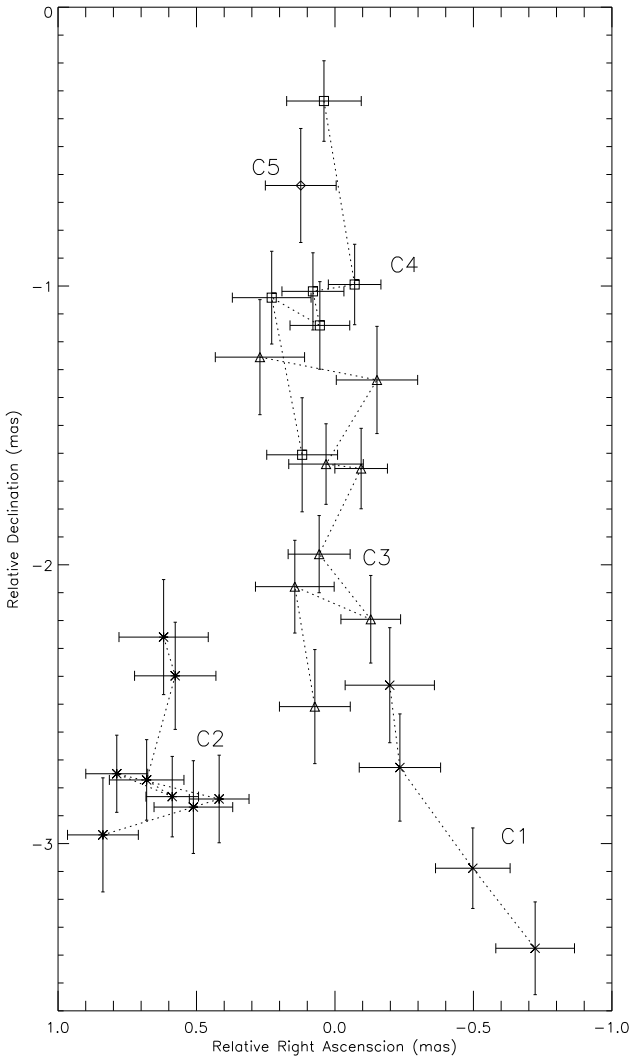

FIG. 5.—Two-dimensional position of every measured component position from every epoch. Dotted lines connect the measurements of each individual component in time sequence. The error bars are one-fourth of the beam FWHM. The crosses represent component C1 (*outer component on right*), the asterisks C2 (*outer component on left*), the triangles C3, the squares C4, and the diamond C5.

to the time between the images. The dotted lines represent the best fit to the component motions, and it is easy to see that the components are moving away from the core.

Note that in the model fits given in Table 2 some of the elliptical components are quite highly elongated, particularly in 1995 January 24 and 1995 October 17. We have investigated the possibility that in these cases the elliptical Gaussians may be better fit by two circular Gaussians or two point sources. This leads to an interpretation with one more inner component and with the two inner components moving outward at uncharacteristically high velocities of order 20 $h^{-1}c$. An important point is that we would not even have seriously considered this interpretation if we had not had such dense time sampling over the last year of observation, and this suggests that the lack of very high velocity components in the compiled data on superluminal sources may in part be a selection effect caused by component misidentification caused by insufficient time sampling. Even though this model with more components leads to interesting conclusions, we have rejected it for several reasons: it is needlessly complex, it gives measured expansion speeds that would place the innermost components in the fastest 1% or so of measured speeds (Vermeulen & Cohen 1994), and it is not supported by the final image. High resolution 43 GHz images of this source also show the same components we identify and support our interpretation of the images (Bloom 1996, private communication).

Figure 5 shows the position on the plane of the sky of every component position at every epoch. As in Figure 3 the error bars are taken to be one-fourth of the beam FWHM. Measurements of individual components are connected by dotted lines to show the time ordering of the points. Note that this plot can be deceptive since the points are not equally spaced in time; apparent motion between two points closely spaced in time is simply caused by the component moving around within the error circle. The spatial coverage of this plot is good; we have thoroughly mapped the geometry of the jet out to 4 mas from the core. Different trajectories for different components are clearly evident; the implications of this structure for the physics of curved jets will be discussed in the next section.

5. DISCUSSION

5.1. *Correlations between Component Ejections and Gamma-Ray Activity*

The recent ejection of components C4 and C5 poses the interesting question of whether the VLBI component ejection may be related to enhanced activity in the γ-ray regime. The one sigma errors on the slope of the line fitted to component C4 in Figure 3 give a time of ejection from the core between 1991 March and 1992 June. This is consistent with the increase in the level of γ-ray activity, which happened between 1992 April and 1992 November, and with the beginning of the radio outburst seen at several frequencies which peaked around 1995 January (see § 2). Since there is only one data point, the velocity of C5 is not determined, but since the other measured velocities are consistent with the inner components having greater apparent speeds, it is reasonable to assume it emerged with a speed equal to the apparent speed of C4, or 11.5 $h^{-1}c$. If we use this velocity along with the one sigma error bars on the one measured position of C5, we get a time of ejection from the core between 1993 October and 1994 December. This is during the time of continuing enhanced γ-ray activity recorded by EGRET. Whether these enhanced levels of γ-ray activity represent discrete flares or a constant higher level of emission cannot be determined from the EGRET light curve. Similar correlations between component ejections and γ-ray activity have been observed for 0528+134 and 3C 454.3 (Krichbaum et al. 1995), 3C 279 (Wehrle et al. 1994), and 0836+710 (Otterbein et al. 1995). Correlations between component ejections and enhanced activity in the optical to radio regions have been observed in many other sources (e.g., Mutel et al. 1990; Zensus et al. 1990), and since such outbursts can occur across the electromagnetic spectrum (e.g., Hartman et al. 1995), the extension of this correlation to γ-rays is not surprising.

EGRET observations of 1611+343 before 1991 do not exist, however it is interesting to compare the estimated ejection times of the older components C1, C2, and C3 with the historical radio and optical light curves. Note however that there is not always a one-to-one correspondence between activity in different spectral regions, and the increased source activity which signals a component ejec-

tion may not be observable at all wavelengths. The radio light curves of 1611+343 since 1980 show no significant structure except for the previously mentioned outburst which peaked around 1995 January. The very low frequency variability seen in this source (e.g., Cotton & Spangler 1978) is not considered here due to the possibility that it is caused by refractive interstellar scintillation (Rickett, Coles, & Bourgois 1984). The optical light curve given in Tornikoski et al. (1994) shows an outburst between 1986 October and 1987 March which may be correlated with the ejection of C3, which has an estimated time range for ejection between 1984 March and 1987 March. The estimated ejection times of C1 and C2 are 1978 April and 1969 May, respectively, before the start of regular radio monitoring of this source. The ranges of possible ejection times for all components along with a listing of possible correlated outbursts are given in Table 3.

5.2. *Calculation of Doppler Beaming Factor*

The VLBI observations can be used to place an upper limit on the angle of the jet to the line of sight, and a lower limit on the Lorentz factor of the components. Although these limits can be obtained by using only the observed superluminal velocities, more stringent limits can be derived if these velocities are compared with a value for the Doppler beaming factor $\delta = [\Gamma(1 - \beta \cos \theta)]^{-1}$. This can be done as long as the motion of the pattern seen in the VLBI images is the same as the bulk motion of the emitting plasma. We use equation (1) of Ghisellini et al. (1993) to derive a lower limit to the Doppler beaming factor. This method uses the observed X-ray flux for the source and assumes that these X-rays are produced by the synchrotron self-Compton (SSC) process. The expected SSC emission from a VLBI component depends on δ and on parameters which can be estimated from the VLBI maps, such as the component size, turnover frequency, spectral index, and flux at the turnover frequency. A lower limit to δ can then be obtained because for values of δ which are too low the calculated X-ray flux from a component is greater than the actual X-ray flux from the source.

We have applied this method to both the core and the jet components. For the jet it would be preferable to obtain a separate spectral index for each component by using the 8 GHz component positions for the 2 GHz model and adjusting the 2 GHz component fluxes (Marscher 1987). However, the resolution of the 2 GHz maps is only sufficient to resolve the core from the jet and not sufficient to distinguish the individual 8 GHz jet components, and this method gives unreasonable results. Therefore we are forced to use one value for the spectral index of the jet for each epoch. Since for the core we are observing below the turnover frequency we must assume an optically thin spectral index of $\alpha = -0.75$. For the core we use a turnover frequency of 10.7 GHz based on single-dish flux measurements (Kühr et al. 1981b). The turnover frequency of the jet is more difficult to estimate; we assume the 2 GHz observations are at the turnover frequency of the jet components, which is the same as deriving a lower limit on δ since δ increases with decreasing turnover frequency. We measure the angular sizes of the components by $\theta = 1.8(\theta_a \theta_b)^{1/2}$, where θ_a and θ_b are the FWHM of the component's major and minor axes (Marscher 1987). Then using an X-ray flux of 0.08 μJy at 1 keV (Dondi & Ghisellini 1995) we obtain an average lower limit from all epochs of $\delta \geq 5.5$ for the average of all jet components and $\delta \geq 8.3$ for the core. The lower limit derived for the core is higher, which probably indicates that the turnover frequency for the core was better estimated. These lower limits are higher than the previously obtained lower limits for 1611+343 of 4.3 (Dondi & Ghisellini 1995) and 2.4 (Biermann et al. 1987).

Lower limits to the Lorentz factors and upper limits to the angles to the line of sight can then be obtained from equations (B5) and (B7) of Ghisellini et al. (1993), with $\delta \geq 8.3$. We obtain $\Gamma \geq 7.1$ and $\theta \leq 6\overset{\circ}{.}8$ for the jet as a whole, by averaging the apparent speeds of all components. For the individual components we obtain $\Gamma \geq 6.9$ and $\theta \leq 6\overset{\circ}{.}8$ for C1, $\Gamma \geq 5.1$ and $\theta \leq 5\overset{\circ}{.}3$ for C2, $\Gamma \geq 7.7$ and $\theta \leq 6\overset{\circ}{.}9$ for C3, and $\Gamma \geq 11.5$ and $\theta \leq 6\overset{\circ}{.}6$ for C4. Since the value of δ used in the calculation is only a lower limit we can not say anything definite about how Γ and θ change among the components, however, the lower limits on Γ suggest that the Lorentz factor of the inner components may be greater than the Lorentz factor of the outer components. Such a decrease in the bulk Lorentz factor of the outer components could be due to a deceleration of the components as they move out or the outer components could simply have been ejected with lower Lorentz factors.

5.3. *Kinematics and Geometry of the Jet*

An important question to answer about blazar jets in general deals with the motion of components in bent or curving jets and whether or not there is a fixed track in each source which successive components follow (Padrielli 1989). The appearance of a curved jet could be caused by different components being ejected along different yet straight trajectories (i.e., ballistic motion). This could occur if the jet is precessing (Begelman, Blandford, & Rees 1980), if the source of the jet is undergoing orbital motion in a binary black hole system (Kaastra & Roos 1992), or if the components are being emitted inside a cone of sizable opening angle (e.g., Readhead et al. 1983). Another alternative is that each component is following the same curved trajectory, where some force is constraining the components to follow a curved path. Helical jets have been proposed to solve the

TABLE 3

COMPONENT EJECTION TIMES

Component	Ejection Time	1 σ Time Range	Corresponding Outbursts[a]
C1	1978 April	1973 July–1981 April	?
C2	1969 May	1955 October–1975 December	?
C3	1986 January	1984 March–1987 March	1986 October–1987 March; optical
C4	1991 December	1991 March–1992 June	1992 April–1992 November; onset of enhanced γ-ray and radio activity
C5[b]	1994 May	1993 October–1994 December	γ-ray activity continues

[a] References discussed in text.
[b] Assuming same velocity as C4.

problem of the large number of sources with 90° misalignments between their parsec- and kiloparsec-scale structure (Conway & Murphy 1993), and helical jet models have been fitted to some sources (e.g., components C4 and C5 of 3C 345; Steffen et al. 1995). The component motion could be more complicated, with individual components following different curved trajectories. Component trajectories which differ from the trajectories of their precursors have been observed for components C6 and C7 in 3C 345 (Krichbaum et al. 1993). In order to answer this question sources with bent jets must be monitored over a long enough time for new components to reach the same distance from the core formerly occupied by the older components. The observations of 1611+343 presented here cover a long enough time span to accomplish this for some of the components.

It can be seen from Figure 5 that the positions of C1 and C2 have been mapped at approximately the same distances from the core, yet they have very different positions and trajectories. This rules out any kind of continuous jet model where each component follows its precursor. A helical jet would not necessarily be expected for 1611+343 since it is a member of the aligned population (Conway & Murphy 1993). The next important question is whether the components follow a fixed straight path out to a certain distance from the core and then bend away to follow the trajectory of C1 or C2, or whether the components start out at the core with their own straight, independent trajectories. If the components do follow a bent path, then since the jet is aligned almost along the line of sight, relatively small intrinsic bends could cause the observed apparent bends; an intrinsic bend of about 4° could cause the observed apparent bend for a jet aligned 6°.5 to the line of sight. Components C3 and C4 define a common path almost due south from the core, and C3 is now far enough out that it is past the earliest observed points for C1 and C2. It is obvious that C3 has not turned to follow C2; the simplest model is that it is continuing straight along its previous path. It is possible that it could still turn to follow C1, although to do so it would have to display a rapid shift toward higher position angles within the next year. Since it is difficult to envision a physical process that would cause a Y-shaped bend in a jet, and since the data are much better fit by independent paths straight out from the core, again we suggest that the most straightforward interpretation of Figure 5 is that each component is ejected from the core with its own independent position angle and that it then moves straight out from the core along this trajectory. Figure 6 shows such trajectories fit to the motion of C1, C2, and of C3, C4, and C5 together. The position angles of these trajectories are $\phi = 167°.3 \pm 0°.9$ for C2; $\phi = 179°.2 \pm 1°.2$ for C3, C4, and C5 together; and $\phi = 188°.7 \pm 1°.4$ for C1.

The mechanism behind these different position angles remains to be explained. Although precession of the jet has been suggested as a mechanism to eject different components along different position angles, the position angles of the components in relation to their order of ejection indicates a timescale much shorter than that suggested for precession (Begelman et al. 1980). It is uncertain from our observations whether C1 or C2 was ejected first, but it is clear that C3, C4, and C5 were ejected after C1 and C2. If the jet was slowly precessing, then C3, C4, and C5 should have been ejected at either lower position angles than C2 or higher position angles than C1, depending on whether C1 or C2 was ejected first. The fact that C3, C4, and C5 are on a

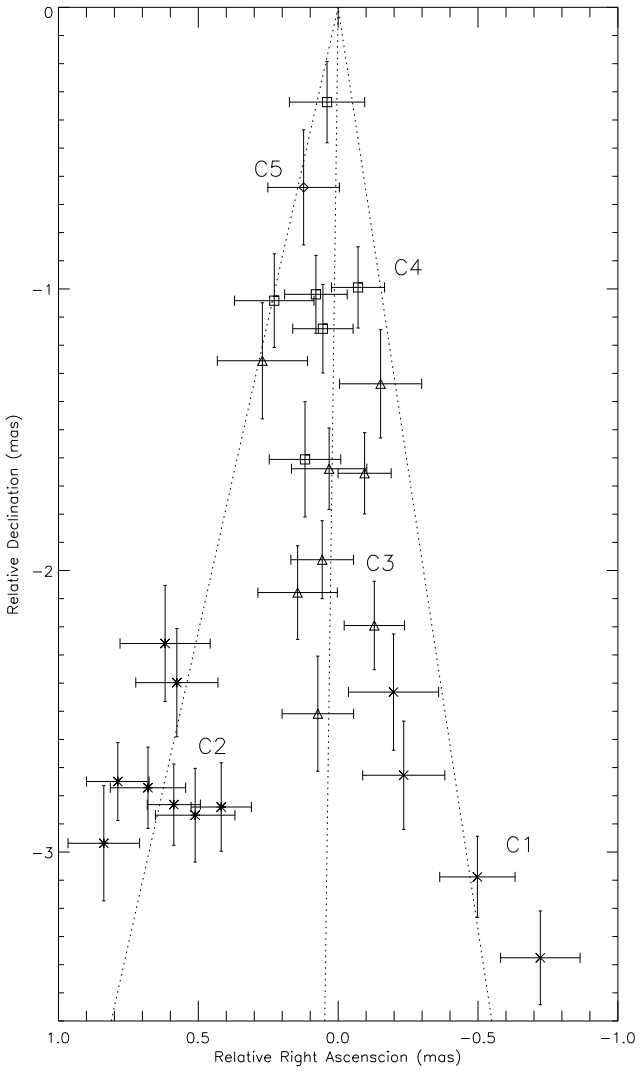

FIG. 6.—Identical to Figure 5 except that instead of the component points being connected in time order, straight trajectories out from the core have been fitted to components C1, C2, and to components C3, C4, and C5 together. The crosses represent component C1 (*outer component on right*), the asterisks C2 (*outer component on left*), the triangles C3, the squares C4, and the diamond C5.

path with a position angle between that of C1 and C2 seems to rule out precession. The timescales suggested for orbital motions in binary black hole systems by Kaastra & Roos (1992) can be much smaller than the precession period and are more consistent with the timescale inferred for 1611+343, so this scenario can not be ruled out.

An alternative to precession or orbital motion is simply that the components are being ejected inside a cone with a sizable opening angle, with the azimuth of the ejection inside the cone being essentially random; however, this possibility has problems as well. If our line of sight to the source lies outside this cone then the cone must have an opening half angle at least 10°.7 to produce the observed differences in position angle between C1 and C2. This angle then conflicts with the upper limit to the angle of the component motions to the line of sight of 6°.5 derived from the X-ray emission. This means that if there is such a cone then our line of sight must lie inside it, and if the azimuth of the ejections inside the cone were truly random we should see components moving in all directions. This scenario requires

an uncomfortable amount of fine tuning: either the azimuth of the ejections favors position angles near 180° or our line of sight must lie barely inside the cone, with the majority of the cone lying to the south of our line of sight. Continued observation over the next several years should be able to settle this problem of component motions. Within 1 yr we should know whether C3 will bend away from its present course to follow C1, and within 2 yr we should have some indication of what will happen to component C4. We are fortunate that the components in 1611+343 have been sufficiently long lived to allow us to study their motions over a time period of 6 yr; components in many sources typically decay with a half-life of 2–3 yr (e.g., Zensus 1987).

5.4. *Superluminal Motion and EGRET Sources*

If relativistic beaming is the correct explanation for apparent superluminal motion, the detection of superluminal motion in 1611+343 confirms the presence of a relativistic jet in this source. Observations of high γ-ray flux from a source actually indicate that the emission must be relativistically beamed in order to avoid photon-photon opacity effects in regions with high photon density (e.g., Jelley 1966). Thus we expect the sample of EGRET sources to display the properties of sources with relativistic jets, including apparent superluminal motion. Superluminal motion has now been confirmed in 15 of the 40 AGNs listed in the second EGRET catalog. Superluminal motion in 10 of these objects is listed in the review by Vermeulen & Cohen (1994) (0735+178, 0836+710, Mrk 421, 1222+216, 3C 273, 3C 279, CTA 102, 3C 454.3, 0716+714 provided its redshift is above the minimum value of 0.28, and possibly 1156+295). Superluminal motion has been discovered more recently in five other EGRET sources: 0420−014 (Wagner et al. 1995), 0528+134 (Krichbaum et al. 1995; Pohl et al. 1995), 0954+658 (Gabuzda et al. 1994), 1633+382 (Barthel et al. 1995), and 1611+343 in this paper. Continued study of these sources with VLBI, as well as continued monitoring across the rest of the spectrum, is important to understand their emission processes.

6. CONCLUSIONS

We have detected apparent superluminal motion of four compact components in the VLBI jet of the EGRET quasar 1611+343. The measured velocities of these four components suggest that the inner components have greater apparent speeds than the outer components. The estimated times of separation from the core of the two youngest components are consistent with a time of enhanced γ-ray activity in this source. We have mapped the geometry of the jet and have found that 1611+343 has one of the more interesting quasar jets. We have observed components that have moved outward to the same distance from the core formerly occupied by older components, and they are clearly on different trajectories from these older components. This rules out a continuous jet model for this source, and, in fact, the present data strongly indicate that components are being ejected from the core at different position angles, and are then moving on straight paths out from the core. Continued VLBI monitoring of this source is important in order to determine whether components C3 and C4 will continue on their present paths.

This paper demonstrates that the pool of EGRET sources which have been relatively sparsely observed with VLBI provides a sample worthy of further study, and it shows that archived geodetic VLBI observations are capable of doing this. Approximately a dozen EGRET sources have enough VLBI data in the database of the Washington VLBI correlator that they can be imaged with comparable quality to 1611+343. Work on imaging these sources is currently underway.

We acknowledge the support of the VLBI staff at the Naval Observatory and the EGRET team at NASA/GSFC. We also acknowledge helpful discussions and communication of data in advance of publication from Steve Bloom, Marshall Eubanks, Bob Hartman, Enrico Valtaoja, Beth Waltman, and Ann Wehrle.

REFERENCES

Aller, H. D., Aller, M. F., Latimer, G. E., & Hodge, P. E. 1985, ApJS, 59, 513
Bååth, L. B. 1987, in Superluminal Radio Sources, ed. J. A. Zensus & T. J. Pearson (Cambridge: Cambridge Univ. Press), 206
Barthel, P. D., Conway, J. E., Myers, S. T., Pearson, T. J., & Readhead, A. C. S. 1995, ApJ, 444, L21
Begelman, M. C., Blandford, R. D., & Rees, M. J. 1980, Nature, 287, 307
Biermann, P. L., Kühr, H., Snyder, W. A., & Zensus, J. A. 1987, A&A, 185, 9
Bondi, M., et al. 1996, A&A, 308 415
Britzen, S., Witzel, A., Gontier, A. M., Schalinski, C. J., & Campbell, J. 1994, in IAU Symp. 159, Multi-Wavelength Continuum Emission of AGN, ed. T. J. L. Courvoisier & A. Blecha (Dordrecht: Kulwer), 423
Carter, W. E., Robertson, D. S., & MacKay, J. R. 1985, J. Geophys. Res., 90, 4577
Charlot, P. 1990, A&A, 229, 51
Clark, T. A., et al. 1985, IEEE Trans. Geosci. Remote Sensing, GE-23, 438
Coates, R. J., Frey, H., Mead, G. D., & Bosworth, J. M. 1985, IEEE Trans. Geosci. Remote Sensing, GE-23, 360
Conway, J. E., & Murphy, D. W. 1993, ApJ, 411, 89
Cotton, W. D., & Spangler, S. R. 1978, ApJ, 228, L63
Dondi, L., & Ghisellini, G. 1995, MNRAS, 273, 583
Eubanks, T. M., et al. 1991, in IERS Technical Note No. 8 (Paris: IERS)
Fiedler, R., Dennison, B., Johnston, K. J., Waltman, E. B., & Simon, R. S. 1994, ApJ, 430, 581
Gabuzda, D. C., Mullan, C. M., Cawthorne, T. V., Wardle, J. F. C., & Roberts, D. H. 1994, ApJ, 435, 140
Ghisellini, G., Padovani, P., Celotti, A., & Maraschi, L. 1993, ApJ, 407, 65
Hartman, R. C., et al. 1995, ApJ, 461, 698
Hewitt, A., & Burbidge, G. 1989, ApJS, 69, 1
Jelley, J. V. 1966, Nature, 211, 472
Kaastra, J. S., & Roos, N. 1992, A&A, 254, 96
Krichbaum, T. P., et al. 1993, A&A, 275, 375
Krichbaum, T. P., Britzen, S., Standke, K. J., Witzel, A., Schalinski, C. J., & Zensus, J. A. 1995, Proc. Natl. Acad. Sci., 92, 11377
Kühr, H., Witzel, A., Pauliny-Toth, I. I. K., & Nauber, U. 1981, A&AS, 45, 367
Marscher, A. P. 1987, in Superluminal Radio Sources, ed. J. A. Zensus & T. J. Pearson (Cambridge: Cambridge Univ. Press), 280
Murphy, D. W., Browne, I. W. A., & Perley, R. A. 1993, MNRAS, 264, 298
Mutel, R. L., Phillips, R. B., Su, B., & Bucciferro, R. R. 1990, ApJ, 352, 81
Otterbein, K., et al. 1995, in preparation
Padrielli, L. 1989, in Very Long Baseline Interferometry: Techniques and Applications, ed. M. Felli & R. E. Spencer (Dordrecht: Kulwer), 319
Padrielli, L., et al. 1986, A&A, 165, 53
Padrielli, L., Eastman, W., Gregorini, L., Mantovani, F., & Spangler, S. 1991, A&A, 249, 351
Pearson, T. J., & Readhead, A. C. S. 1984, ARA&A, 22, 97
Piner, B. G., & Kingham, K. A. 1997, in preparation
Pohl, M., et al. 1995, A&A, 303, 383
Readhead, A. C. S., Hough, D. H., Ewing, M. S., Walker, R. C., & Romney, J. D. 1983, ApJ, 265, 107
Rickett, B. J., Coles, W. A., & Bourgois, G. 1984, A&A, 134, 390
Rogers, A. E. E., et al. 1983, Science, 219, 51
———. 1993, in Geodynamics Ser. 25, Contributions of Space Geodesy to Geodynamics: Technology, ed. D. E. Smith & D. L. Turcotte (Washington,DC: AGU),47
Romney, J. D., et al. 1984, A&A, 135, 289
Rusk, R. E. 1988, Ph.D. thesis, Univ. Toronto
Rusk, R. E., & Seaquist, E. R. 1985, AJ, 90, 30

Smith D. E., & Turcotte, D. L., ed. 1993, Geodynamics Ser. 23, Contributions of Space Geodesy to Geodynamics: Crustal Dynamics (Washington: AGU)
Steffen, W., Zensus, J. A., Krichbaum, T. P., Witzel, A., & Qian, S. J. 1995, A&A, 302, 335
Thompson, D. J., et al. 1995, ApJS, 101, 259
Tornikoski, M., Valtaoja, E., Teräsranta, H., Smith, A. G., Nair, A. D., Clements, S. D., & Leacock, R. J. 1994, A&A, 289, 673
Vermeulen, R. C., & Cohen, M. H. 1994, ApJ, 430, 467
von Montigny, C., et al. 1995, ApJ, 440, 525
Waak, J. A., Spencer, J. H., Simon, R. S., & Johnston, K. J. 1988, in IAU Symp. 129, The Impact of VLBI on Astrophysics and Geophysics, ed. M. J. Reid & J. M. Moran (Dordrecht: Kulwer), 95
Wagner, S., et al. 1995, A&A, 298, 688
Waltman, E. B., Fiedler, R. L., Johnston, K. J., Spencer, J. H., Florkowski, D. R., Josties, F. J., McCarthy, D. D., & Matsakis, D. N. 1991, ApJS, 77, 379
Wehrle, A. E., et al. 1994, in The Multimission Perspective (Napa Valley, CA: Eureka Scientific), 27
Xu, W., Readhead, A. C. S., Pearson, T. J., Wilkinson, P. N., & Polatidis, A. G. 1994, in NRAO Workshop 23, Compact Extragalactic Radio Sources, ed. J. A. Zensus & K. I. Kellermann (Green Bank: NRAO), 7
Zensus, J. A. 1987, in Superluminal Radio Sources, ed. J. A. Zensus & T. J. Pearson (Cambridge: Cambridge Univ. Press), 26
Zensus, J. A., & Pearson, T. J. 1988, in IAU Symp. 129, The Impact of VLBI on Astrophysics and Geophysics, ed. M. J. Reid & J. M. Moran (Dordrecht: Kulwer), 7
Zensus, J. A., Porcas, R. W., & Pauliny-Toth, I. I. K. 1984, A&A, 133, 27
Zensus, J. A., Unwin, S. C., Cohen, M. H., & Biretta, J. A. 1990, AJ, 100, 1777